Lateral Diffusion of an 80,000-dalton Glycoprotein in the Plasma Membrane of Murine Fibroblasts: Relationships to Cell Structure and Function

KENNETH JACOBSON, DONNA O'DELL, and J. THOMAS AUGUST
Laboratories for Cell Biology, Department of Anatomy and Cancer Research Center, School of Medicine, University of North Carolina at Chapel Hill 27514; Department of Pharmacology and Experimental Therapeutics, The Johns Hopkins University School of Medicine, Baltimore, Maryland 21205

ABSTRACT The lateral diffusion of an 80,000-dalton major cell surface glycoprotein of murine fibroblasts has been measured. This antigen, identified through the use of monoclonal antibodies, is an integral glycoprotein distributed through the plasma membrane as judged by immunofluorescence and immunoelectron microscopy (see preceding paper). Measurements of fluorescence recovery after photobleaching were performed on the antigen-antibody complex within the plasma membrane of C3H/10T½ and NIH/3T3 cells after labeling the monoclonal antibody with fluorescein. Measurements were performed as a function of temperature, for interphase, mitotic, and G_0 C3H/10T½ cells. The mean lateral diffusion coefficients (D) for the antibody-protein complex in interphase cells were in the range of 0.7–3.5 × 10^{-10} cm^2/s between 9° and 37°C, while that for the lipid analog probe, dihexadecylindocarbocyanine was about two orders of magnitude greater. This comparison indicates that peripheral interactions other than bilayer fluidity limit the lateral mobility of the antigen. The mobile fraction of mitotic, G_0, and interphase cells showed a monotonic increase with temperature with most of the antibody-antigen complexes being free to move about 25°C. Semi-quantitative interpretations of both the slow glycoprotein diffusion and the immobile fraction are offered. Comparison of diffusion coefficients for cells in different phases of the cell cycle does not reveal striking differences. Mobile fractions for G_0 cells at 25°C or less are substantially lower than in interphase cells. In all cases, there was a remarkably broad range of the fluorescence recovery data between different cells, resulting in up to a 10-fold variation in diffusion coefficients, which is far greater than the precision limits of the experiment. Diffusion values and mobile fractions were generally well within a factor of two when measured at several arbitrary points on a single cell. The origins of this cellular heterogenity remain to be elucidated. Lateral mobility in cell fragments and specific regions of single cells was also examined. The glycoprotein was mobile in ventral surface cell fragments. Its mobility was not altered in regions of cell-cell underlapping. However, the diffusion coefficient was threefold higher near the leading edge of motile cells compared to the trailing region. This difference may reflect weaker coupling of the glycoprotein to the underlying cytoskeleton in the dynamic leading edge region.

Photobleaching techniques have been used to measure the lateral diffusion of cell surface proteins and glycoproteins in a variety of cellular plasma membranes and even some endomembranes (1). One aim of these studies is to understand the physical and biological factors that determine the magnitude of the lateral diffusion rates and the biological role of such mobility. The important observations in plasma membranes have been that the lateral diffusion rates of membrane proteins are considerably slower than expected based on experiments with membrane proteins reconstituted into bilay-

THE JOURNAL OF CELL BIOLOGY · VOLUME 99 NOVEMBER 1984 1624–1633

ers, and that a significant fraction of each protein population measured is immobile on the time scale of the determination (for review, see reference 2). Progress toward understanding the origin of the slow rates of diffusion and the presence of an immobile fraction has been made with the erythrocyte membrane. The spectrin matrix underlying the plasma membrane has been quite convincingly implicated in restricting the lateral mobility of the band 3 proteins (3, 4). Progress also has been made on nucleated cells where diffusion measurements on membrane "blebs" largely free of membrane associated cytoskeleton show enhanced lateral mobility of various proteinaceous receptors (5, 6).

The research presented in this and the previous paper was designed to obtain the lateral distribution and baseline lateral mobility values for a single antigenic entity on the surface of nucleated cells. Previous studies have identified a series of surface antigens from mouse embryo 3T3 cells, one of these being an 80,000-dalton glycoprotein (7). This glycoprotein was a predominant iodinated component of the 3T3 cell surface with $\sim 10^6$ antigenic sites distributed throughout the surface of the NIH/3T3 cell (8). Work described and cited in the preceding paper showed that this antigen redistributed during cell motility and very likely is involved in cell-cell adhesion. Furthermore, this work also showed that normal cellular function was not grossly altered when these monoclonal antibodies bound to this cell surface antigen. These combined findings made a detailed photobleaching study highly desirable in this cell system.

MATERIALS AND METHODS

Reagents and cell culturing techniques were described in the previous paper.

Synchronization of Cell Cultures: C3H/10T½ cells were synchronized by first arresting the cells in G_0 through serum deprivation and then stimulating the cells to re-enter the cell cycle through serum replacement. Cells were seeded onto coverslips at a density of 5×10^4 cells per 35-mm petri dish in enriched basal medium Eagle (BME)[1] (containing L-glutamine and antibiotic-antimycotic solution) plus 5% fetal bovine serum (FBS). After 12 to 24 h, the cell monolayers were rinsed three times with PBS and fed with enriched BME plus 1% FBS. The cells were monitored for entry into G_0 by daily cell counts. The total number of cells per 35-mm petri dish was counted with a hemacytometer following removal of the cells by trypsinization. At least two separate counts from each of two duplicate dishes were averaged to give the mean cell number for each day. When the total cell number did not increase significantly in a 2–3-d period, the cells were assumed to be in G_0. The plateau in total cell number usually occurred after 72 to 96 h in low serum, at which time there was no further increase in cell number. After the cells were determined to be in G_0, they were stimulated to re-enter the cell cycle by replacing the low-serum media with enriched BME supplemented with 15% FBS. Following serum stimulation, the cells entered an extended G_1 phase; the cells began to enter S phase ~12 h after the addition of the BME plus 15% FBS.

Autoradiography of parallel cultures was performed to confirm that these growth arrested cells were actually in the G_0 phase of the cell cycle and to determine when the stimulated cells were entering S phase. Cultures in 35-mm petri dishes were pulsed for 1 h with 5 μCi tritiated methyl thymidine (Research Products International, Mount Prospect, IL) injected into the media. The cells were then quickly rinsed twice with PBS and fixed in methanol (2 × 10 min, at room temperature); after extensive rinsing with tap water, the cells were allowed to air dry. The cells were coated with NTB2 nuclear track emulsion (Eastman Kodak, Rochester, NY) and dried for at least 2 d in a light-tight box containing drierite. The autoradiographs were developed in Microdol X (Eastman Kodak), rinsed in distilled, deionized H_2O (ddH_2O), and fixed with Rapid Fixer (Eastman Kodak). Following a brief (3–5 min) rinse in tap water, the autoradiographs were stained with Giemsa. At least 200 cells were scored as having either labeled or unlabeled nuclei; all percentages are the average values for duplicate cultures.

[1] *Abbreviations used in this paper:* diI-C_{16}(3), dihexyadecylindocarbocyanine; FRAP, fluorescence recovery after photobleaching; GP80, major 80,000-dalton murine cell surface glycoprotein; mf, mobile fraction.

Fluorescence Recovery After Photobleaching: The microscope for photobleachng has been previously described in detail (9). The relatively low light levels provided by the direct immunofluorescence staining were measured with a × 40 phase contrast 1.3 NA oil immersion objective with a focused laser beam radius, w_0, of 1.05 μm. The beam radius was measured and calculated as described before (10). The contribution from residual substrate fluorescence was reduced by use of a 350-μm image plane diaphragm positioned in a Leitz MPV-1 photometer head.

Cells were labeled with 25 to 100 μg/ml dichlorotriazinylaminofluorescein (DTAF) conjugated anti-GP80 (αGP80), washed in PBS, and mounted as described below. Because the anti-GP80 stain was faint and because both fluorescein isothiocyanate (FITC) and dichlorotriazinylaminofluorescein conjugates fade very rapidly, several precautions were taken to avoid unnecessary photobleaching of the specimen. Labeling of the cells with the antibody was performed in a dimly lit room; cells to be photobleached were located and positioned using phase microscopy.

Defocusing of the specimen during fluorescence recovery after photobleaching (FRAP) experiments was avoided by mounting cells grown on coverslips on stainless steel chambers designed by Dr. Albert Harris (University of North Carolina, Chapel Hill). The 7.0 × 3.5-cm stainless steel slides varied in thickness from 1.5 mm for normal use to 0.18 mm for use with the temperature stage. Each slide had a hole 1.55 cm in diameter in its center; a 24 × 50-mm glass coverslips was affixed to one side of the slide with sticky wax (Sybron/Kerr, Emeryville, CA); the chamber so formed was filled with PBS. The coverslip with the cells on it was then mounted on the slide cell side down centered over the chamber; the coverslip was secured by a thin layer of high vacuum grease (Dow Corning, Midland, MI) between it and the slide.

FRAP measurements at temperatures other than room temperature were conducted with a thermoelectric temperature stage (Bailey Instruments, Saddlebrook, NJ). An air curtain incubator (Sage Instruments, Division of Orion, Cambridge, MA) was also required to achieve 37°C. The actual temperature of the cells during a FRAP experiment was determined by measuring the temperature with a thermocouple microprobe (Bailey Instruments) mounted on a blank stainless steel chamber identical to that used for the cells and placed on the temperature stage with the microscope objective in position to accurately simulate the experimental thermal geometry.

Measurements were routinely made over the cytoplasm in distal portions of well spread cells so as to avoid reddish-yellow perinuclear autofluorescence often observed in the C3H/10T½ cells. Any autofluorescence and background fluorescence in this region of the cell was corrected for by subtracting the fluorescence intensity in similar regions on unstained cells. Background fluorescence was <10% of the total signal.

Data Processing: Given the relatively low signal to noise ratio of spot photobleaching measurements involving 10^6 receptors per cell, the question arises of how to fit the individual recovery curves. We examined this question in some detail using nonlinear least squares computer modeling (11), based on the analysis of Axelrod et al. (12). A two parameter (one diffusing component, one immobile component) model was compared with a three parameter (two populations of diffusing species and a partition coefficient) model. We adopted the following criteria for comparing the two parameter and three parameter models. The two models were considered to be equally valid (i.e., to provide identical fits to the data) if: (*a*) for nearly complete recoveries, the two diffusion coefficients (D) in the three parameter fit differed by less than a factor of two or if the two D's differed by more than a factor of two, one population was ≤15%. (*b*) When full recovery was not obtained, agreement of the two models was defined if the three parameter fit returned a fraction of slow diffusion component, i.e., $D \leq 10^{-30}$ cm²/s, within ± 10% of the immobile fraction in the two parameter fit. 19 recovery curves were analyzed by these criteria; 11/19 recoveries were explained in a similar fashion by both models. The curve fitting statistics were similar for both models in the remaining cases, indicating the two models gave satisfactory but differing fits to the data; however, in only one case, did the partial F-test justify the addition of the third parameter to a 90–95% confidence level. Thus, given our typical signal to noise ratio, the data were consistent with the two parameter model consisting of a diffusing and a nondiffusing fraction.

The visual fitting of the data employing the series solution for diffusive fluorescence recovery (12) computed by a hand calculator gave results that agreed with the two parameter model calculated by computer. The mean difference between the calculator fitting and the computer fitting was ~20% for both D and mf values.

Our procedure was then to first discard the few runs in which an obviously nondiffusive recovery had occurred (possibly due to cell motion) and then to calculate D for the mobile fraction from the measured recovery half-time ($\tau_{1/2}$). This D value was then checked to see that it yielded a theoretical recovery curve consistent with the measured data.

The Fading Problem: One systematic problem with FRAP experiments, particularly with fluorescein conjugates, is that of fading during the

measurement phase. We have found empirically that fading is a biphasic process with initial rates of fading approaching a 20% loss of intensity per second; the rates after the major photobleaching are often too small to measure accurately. This means that each interrogation pulse is another bleaching experiment with an attendant minor recovery in addition to that caused by the major bleach pulse. The minor recovery after each measuring pulse will occur to an extent dependent on the time between pulses. An approximation to the systematic error generated by fading can be made by calculating the deviation from theoretical recovery caused by the measuring beam bleaching and minor recovery. Intuitively, fading reduces the mobile fraction and shortens the apparent $\tau_{1/2}$ because recovery no longer reaches its full extent. Thus, lateral diffusion constants calculated from the $\tau_{1/2}$ (12) will give values that are systematically too high.

We constructed a fading model that incorporates the length of each measuring pulse and the interval between measuring pulses, by which the effect of fading can be simulated. We have used two measuring protocols: in our standard protocol *A* 0.85 s measuring pulses are taken at 0, 4, 12, 28, 44, and 60 s, and then every 32 s until the run is terminated; in protocol *B*, a more restricted sampling of the FRAP curve is made at 0, 16, 48, 80, and 112 s, and then at 300–600 s to determine the final extent of recovery (F_∞). If such measuring protocols are incorporated into the fading model calculated for a D of 10^{-10} cm^2/s and a 100% mobile fraction (mf), it can be calculated that protocol *A* yields a D value (1.15×10^{-10} cm^2/s) 15% too high and an mf of 80%, while protocol *B* yields a D of 1.05×10^{-10} cm^2/s and an *mf* of 86%. Thus, these estimations suggest that the systematic effect of fading will not significantly perturb the conclusions of these studies. Actual experiments comparing the two protocols, at different spots on the same cell, yielded very little difference between the results obtained with either of them.

RESULTS

Lateral Mobility of the Antigen-Antibody Complex

ANTIBODY BINDING: A persistent question in cell surface photobleaching is how tightly does the antibody bind to the antigen. We approached this question by measuring the amount of fluorescence remaining after both simple washing (to remove dissociated antibody) and by competitive replacement of labeled antibody with unlabeled antibody. The former is a fairer test for divalent antibodies since, in the competition assay, unlabeled antibody may prevent the reassociation of the labeled antibody that had detached from one binding site. Table I shows that at 24°C, unlabeled antibody elutes fluorescent anti-GP80 off the cell surface but on a time scale (half-time >30 min) much longer than a typical FRAP determination ($\tau_{1/2} \approx 30$ s). At 37°C, the dissociation of the antibody from the cell surface after washing is still slow (half-time >30 min) (Table II). The very long persistence binding seen in Fig. 4 of the preceding paper indicates the presence of a class or classes of even higher affinity binding.

TABLE I

Competitive Replacement of DTAF anti-GP80 with Unconjugated anti-GP80 from the Surface of C3H/10T½ Cells at 25°C

Staining conditions*	Mean fluorescence by spot photometry of single cells‡
Control stain	6.57 (± 0.32)
Control stain followed by 5 min incubation with anti-GP80	6.52 (± 0.72)
Control stain followed by 30 min incubation with anti-GP80	4.93 (± 0.42)

* Control stain was a 5 min incubation with 100 μg/ml of dichlorotriazinylaminofluorescein-anti-GP80 followed by washing; competitive inhibition of this stain was accomplished by incubating the labeled cells with 100 μg/ml of unlabeled anti-GP80 for the specified times.

‡ Intensity (± SEM) was measured with the measuring beam of the FRAP microscope using a × 40 (1.3) objective; laser beam diameter on the specimen (2 w_s) ~2.1 μm.

TABLE II

Dissociation of DTAF anti-GP80 Bound to the Surface of C3H/10T½ Cells

Treatment*	Mean fluorescence‡ after treatment
Control stain	4.81 (± 0.28)
Dissociation after 5 min	
at 25°C	4.39 (± 0.47)
at 37°C	4.10 (± 0.34)
Dissociation after 30 min	
at 25°C	3.93 (± 0.48)
at 37°C	3.46 (± 0.36)

* Control stain as in Table I; dissociation assayed by measuring the amount of fluorescence remaining after incubation in PBS for the times and temperatures indicated followed by washing out the dissociated antibody.

‡ Intensity (± SEM); measured as described in Table I.

Lateral Diffusion Results as a Function of Temperature and Phase in the Cell Cycle

Histograms of the diffusion coefficients (D) and mobile fraction (*mf*) of the protein-antibody complexes are given (Figs. 1 and 2) as a function of temperature for interphase, mitotic, and G_0 cells. A broad range of D values roughly centered around 10^{-10} cm^2/s with a positive temperature coefficient was obtained (Fig. 1, Table III). The distribution of values appears to be bimodal particularly for interphase cells at 37°C. The cell to cell range of values (an order of magnitude) significantly exceeds the variation of values obtained by bleaching two spots on the same cell, which usually differ by less than a factor of two (Fig. 3, *lower*). The mf values showed a positive temperature coefficient with many cells displaying nearly 100% recovery at 37°C for both interphase and mitotic cells (Fig. 2, Table IV). Also, mobile fractions measured at arbitrary positions within the same cell are nearly equal (Fig. 3; *upper*).

Mean values of each distribution are plotted vs. temperature for D (Fig. 4). Data for the lateral diffusion of the lipid analog, dihexadecylindocarbocyanine ($diIC_{16}(3)$) in interphase C3H/10T½ cells is also plotted (Fig. 4, top curve). Lipid probe diffusion is approximately two orders of magnitude faster than the protein-antibody complexes in the plasma membrane of interphase cells.

The mean values for mf show a pronounced positive temperature dependence (Fig. 5). Values of the mf approach 80% at 37°C for interphase cells; these are among the highest values recorded for cell surface glycoproteins. G_0 cells display a depressed mf, most notably at 24°C.

FRAP results with NIH/3T3 cells at room temperature are similar to those with C3H/10½ cells; however, because the NIH/3T3 cells are less well spread and have a higher autofluroescence background throughout the cytoplasm, they are less suitable for the photobleaching studies.

Lateral Diffusion in Different Regions of Single Cells

FRAP results with ventral surface fragments yielded diffusion coefficients of ~4×10^{-10} cm^2/s and mobile fractions of ~50% at 24°C (data not shown). We have previously shown

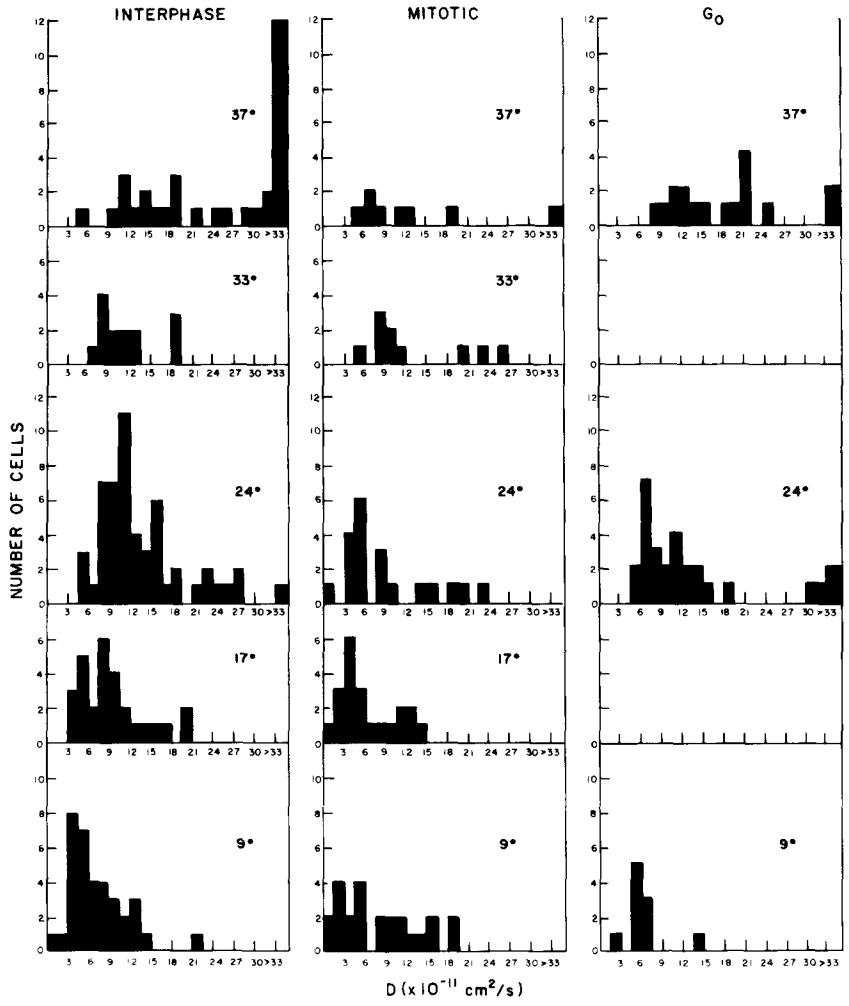

FIGURE 1 Distribution of calculated diffusion coefficients for the anti-GP80–GP80 complex in the plasma membrane of interphase, mitotic, and G_0 C3H/10T½ cells. Temperatures indicated on each panel. 40× (1.3 NA) objective employed with an e^{-2} beam radius of ~1.05 μm. Bleach power, ≈2 mW; bleach time, ≈20 ms. Attenuation for measuring beam, ≈10^4.

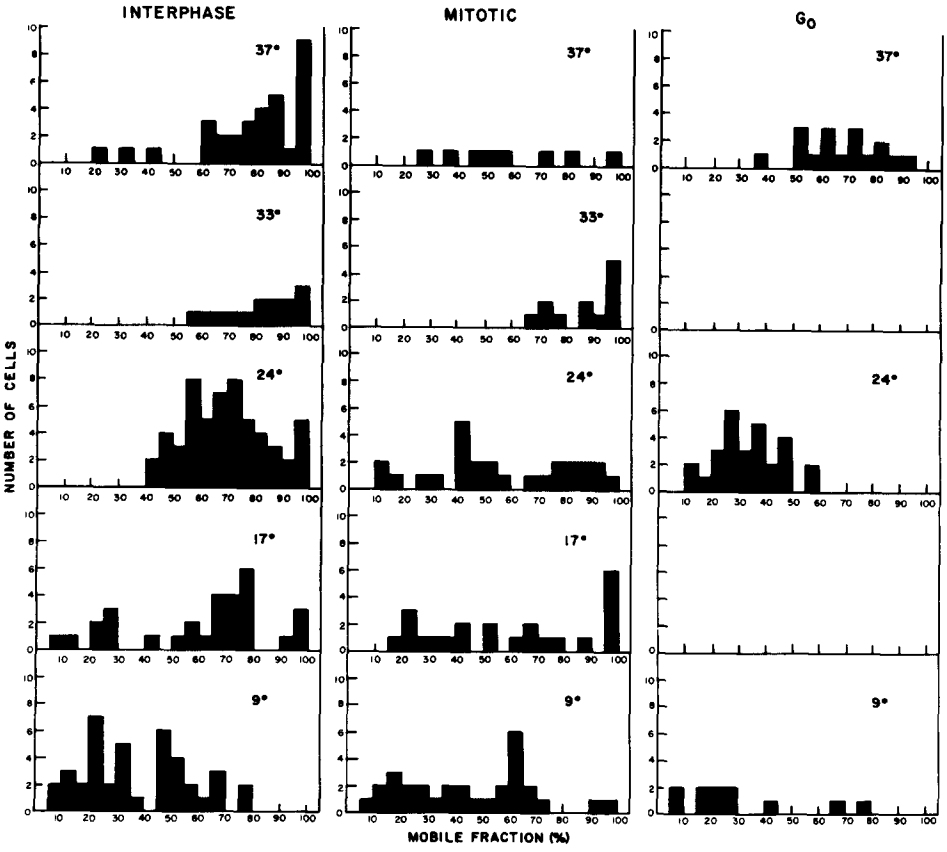

FIGURE 2 Distribution of mobile fractions (% recovery) for the anti-GP80–GP80 complex in the plasma membrane of interphase, mitotic, and G_0 cells. Temperatures indicated on each panel; measurement conditions same as described in Fig. 1.

TABLE III

Lateral Diffusion of Antibody-GP80 Complexes during Various Phases of the C3H/10T½ Cell Cycle

Phase of the cell cycle	Diffusion coefficient (± SEM) in cm^2/s		
	9°C	24°C	37°C
Interphase	$7.3 (\pm 0.7) \times 10^{-11}$	$1.4 (\pm 0.1) \times 10^{-10}$	$3.2 (\pm 0.4) \times 10^{-10}$
Mitotic	$8.0 (\pm 1.1) \times 10^{-11}$	$8.6 (\pm 1.4) \times 10^{-11}$	$1.7 (\pm 0.4) \times 10^{-10}$
G_0	$6.4 (\pm 0.9) \times 10^{-11}$	$1.4 (\pm 0.2) \times 10^{-10}$	$2.3 (\pm 0.5) \times 10^{-10}$

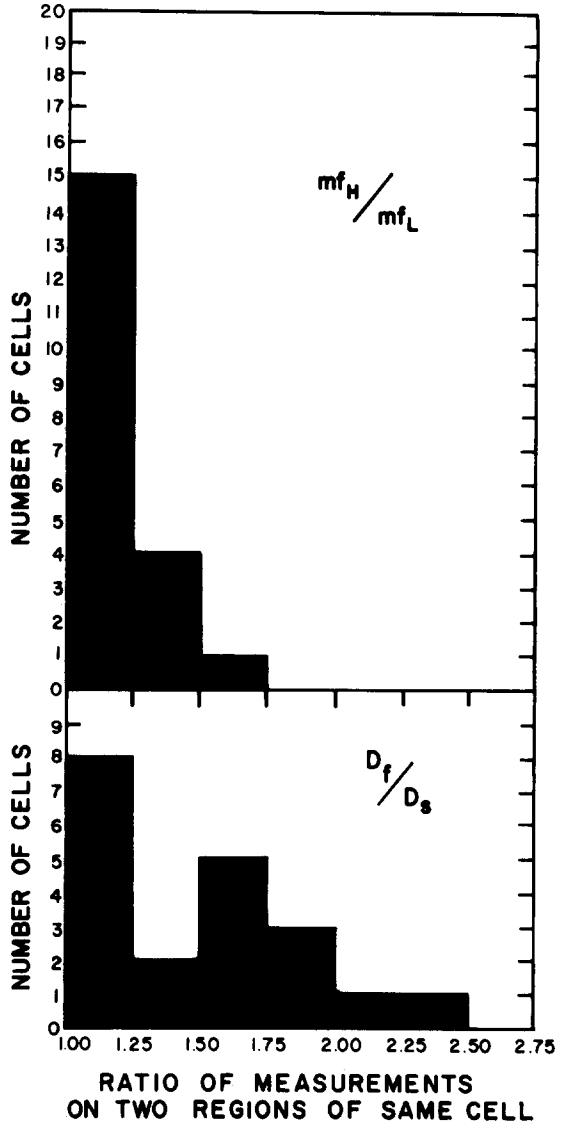

FIGURE 3 Ratio of measurements in two arbitrary regions of the same cell. *Top*, ratio of higher mobile fraction (mf_H) to lower mobile fraction (mf_L); *bottom*, ratio of faster D (D_f) to slower D (D_s).

TABLE IV

Mobile Fraction of Antibody-GP80 Complexes during Various Phases of the C3H/10T½ Cell Cycle

Phase of the cell cycle	Mobile fraction (± SEM)		
	9°C	24°C	37°C
	%	%	%
Interphase	38 (± 3)	70 (± 2)	79 (± 4)
Mitotic	45 (± 4)	54 (± 5)	59 (± 9)
G_0	29 (± 7)	34 (± 2)	67 (± 3)

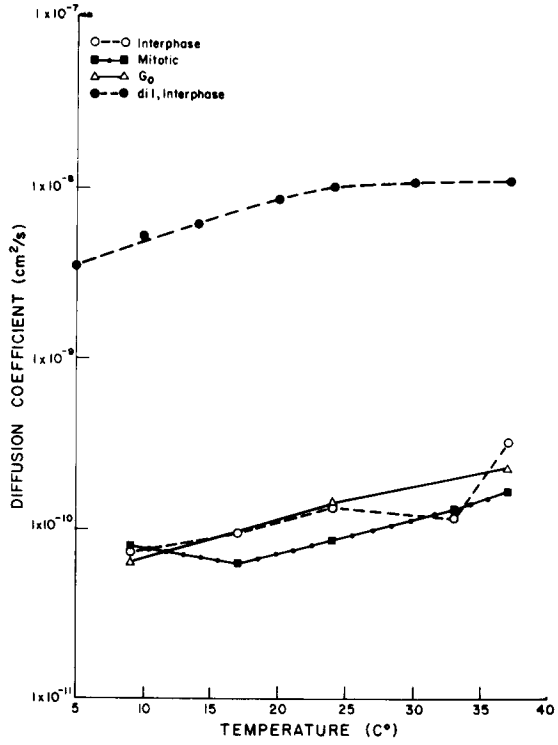

FIGURE 4 Mean value of the lateral diffusion coefficient of anti-GP80–GP80 complex and dil-C_{16}(3) as a function of temperature in the C3H/10T½ cell plasma membrane. O, anti-GP80–GP80 diffusion coefficients in interphase cells; ■, in mitotic cells; Δ, in G_0 cells; ●, dil-C_{16}(3) diffusion coefficients in interphase cells.

that dil-C_{16}(3) would stain bottom surface fragments of human fibroblasts; lipid analog diffusion on such fragments was similar to that measured in intact cells (10).

GP80 lateral diffusion was unaffected by cell-cell contact in regions of underlapping (Fig. 6). Neither the D or mf was altered by such contact; as expected, fluorescence intensity was approximately doubled where one cell underlapped another.

We examined GP80 lateral diffusion near the leading edge compared with the trailing edge of motile fibroblasts and observed a significant increase (threefold) in the D value in the region of the leading edge (Fig. 7). Also, the antigen density in the leading edge was about half that in the trailing edge region as judged by the fluorescence intensity (see preceding paper).

DISCUSSION

Data Interpretation

There are several considerations in interpreting FRAP data from protein-antibody complexes located in cell surface mem-

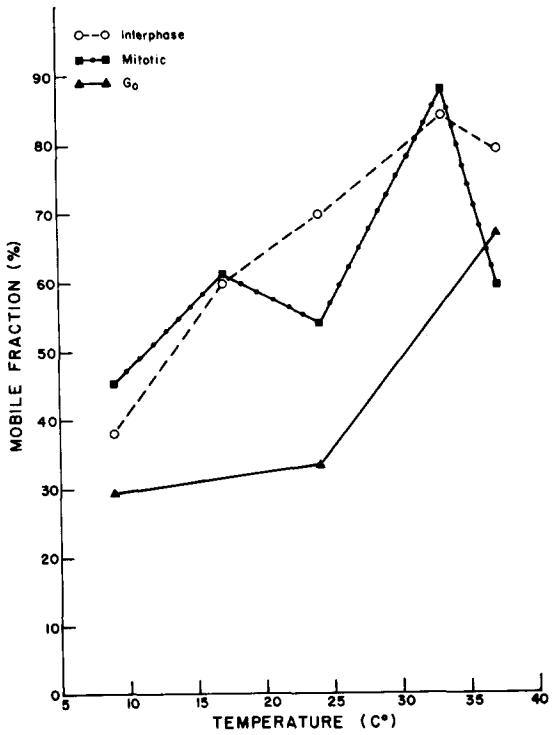

FIGURE 5 Mean value of the mobile fraction of the anti-GP80–GP80 complex and dil-C_{16}(3) as a function of temperature in the C3H/10T½ cell plasma membrane. O, interphase cells; ■, mitotic cells; Δ, G_0 cells.

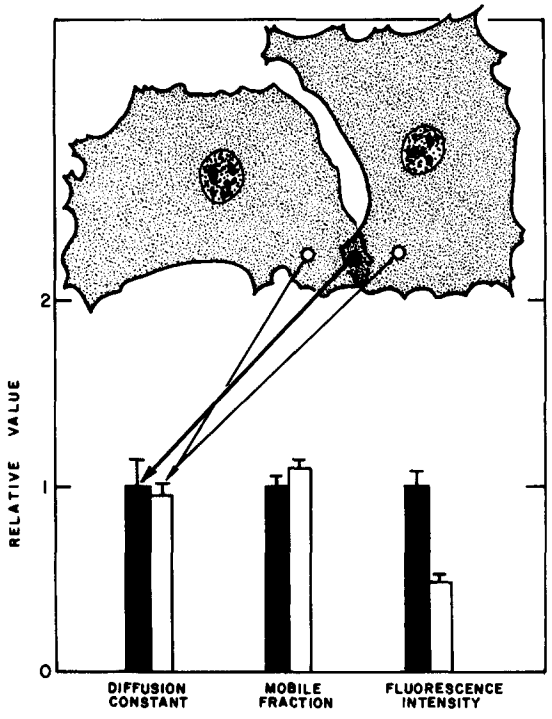

FIGURE 6 Relative D and mobile fraction for anti-GP80–GP80 complexes in regions of cell overlap (dark bar) and free surface (open bar). Contact region set arbitrarily to one. Bars at right give relative fluorescence intensity for spots within and outside of contact region. Laser spot diameter ≈2 μm; measurement conditions as in Fig. 1.

branes. Major photodamage artefacts during photobleaching seem to be excluded by several indirect (13) and elegant direct tests (14, 15). The influence of the divalent antibody on

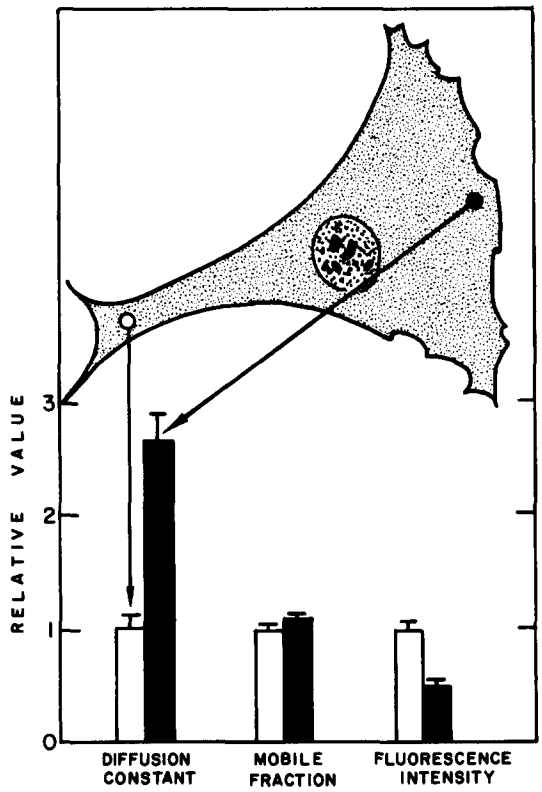

FIGURE 7 Relative D and mobile fraction for anti-GP80–GP80 complexes in leading edge (dark bar) vs. trailing portion (open bar) in motile C3H/10T½ fibroblasts at 25°C. Values for trailing edge arbitrarily set to 1. Bars at right show relative fluorescence intensity and indicate the decreasing antigen surface density toward the leading edge (see preceding paper). Laser spot diameter ≈2 μm; measurement conditions as in Fig. 1.

antigen diffusion poses a possible interpretational problem. In the preceding paper, we have given fluorescence microscopic and ultrastructural evidence to suggest that antigen "patching" does not occur on the cell surface after staining with anti-GP80. A similar result was obtained with a monoclonal anti-H-2 where the fluorescence was uniform whether the intact antibody or its Fab fragment was employed to label the antigen on the cell surface (M. Edidin, personal communication). In addition, the Thy 1.1 antigen on the surface of rat fibroblasts was only patched by a second antibody directed to the anti-Thy 1.1 (15a). Also, anti-HLA (IgG) patterns were uniform on lymphocytes and the antibody-antigen complexes were mobile in half of the cells; however, the same monoclonal antibody caused rapid patching of the antigens on monocytes and polymorphonuclear leukocytes (16). Monoclonal antibody to the G glycoprotein of vesicular stomatitis virus when added to infected Friend erythroleukemia cells caused patching of the cell surface G protein which could be alleviated by using Fab fragments of the antibody (Puddington, L., D. Lyles, K. Jacobson, and J. Parce; unpublished experiments); this result could be anticipated on the basis that G exists as a (multivalent) trimer in the membrane. Thus, it appears that if monoclonal antibodies interact as multivalent ligands with surface antigens bearing more than one identical binding domain, visible "patching" occurs, whereas if they can only interact in a simple uni- or divalent manner, uniform distribution of antigen is maintained and the lateral mobility will be similar whether measured by the intact IgG or its Fab fragment. In general, these findings agree with binding studies

of monoclonal antibodies to surface antigens of rat and mouse thymocytes which have revealed a substantial amount of univalent binding (≈50%) for high affinity antibodies (17).

A second issue is the dissociation rate of the antibody and the possible "hopping" from antigen to antigen during the FRAP measurement. Washing the cells or adding unlabeled antibody for 5 min at 25° and 37°C did not remove appreciable amounts of labeled antibody. Some depletion of labeled antibody occurred after 30-min treatments; however, antibody did remain bound to the antigen for half-times in excess of the 5 to 10 min required to complete the FRAP determination. Edidin and Wei (18) have reported a similar control experiment showing that surface bound monoclonal anti-H-2 Fab's were not removed with unlabeled antibody on a time scale comparable to the FRAP experiment. These experiments are also qualitatively compatible with the half-times for dissociation reported for monoclonal antibody binding to cell surface antigens of rat thymocytes. Mason and Williams (17) have measured half-times ranging from ~500 s at 37°C (for Fab fragments) to ~30,000 s at 6°C; as expected, longer half times were found for the divalent $F(ab)_2$ fragments. These lines of evidence strongly suggest that many monoclonal antibodies remain bound to cell surface antigens for times in excess of that required for a photobleaching determination of the lateral mobility of the antibody-antigen complex.

Another possible complication is the influence of the antibody ligand on the diffusion of the antigen. Poo (19) has shown that the recovery of acetylcholine sensitivity presumably due to the lateral diffusion of non-liganded acetylcholine receptors into a small region inactivated by a localized application of α-bungarotoxin yields receptor lateral diffusion coefficients up to 100-fold larger than those obtained by photobleaching (20) although later measurements reduced this discrepancy somewhat (Poo, M. M., and D. Axelrod, personal communication); nevertheless, the discrepancy raises the question of the effect of the ligand, rhodamine-α-bungarotoxin, on the photobleaching result. On the other hand, slow diffusion has also been observed when small fluorophores are used as glycoprotein tags in erythrocyte membranes (3, 4) and the membranes of tissue culture cells (21, 22). Furthermore, cell surface proteins labeled with antibodies (or FAB fragments) directed toward covalently attached trinitrophenol moieties yielded similar results as direct labeling with a small fluorophore (21). These results argue against a significant perturbation of the antigen diffusion rate by the presence of the antibody.

Glycoprotein Lateral Diffusion

The mobility of a number of specific cell surface proteins has been measured using the photobleaching techniques. These include, for example, the IgE receptor on mast cells (23), the acetylcholine receptor on myoblasts (20), surface Ig receptors on lymphocytes (24, 25), the epidermal growth factor receptor (26), and cell adhesion molecules (27). Recently, monoclonal antibodies have been used to label human (16) and murine (18) histocompatibility antigens and to measure the mobility of the resultant antibody-antigen complexes. All of these results have yielded ligand receptor lateral diffusion coefficients in the range of $0.5\text{–}6 \times 10^{-10}$ cm^2/s and mobile fractions <100% (2). The D values for GP80 fall into this range and are ~100-fold lower than those for the lipid probe, dil (Fig. 4). Similar comparisons have been made previously (see, for example: 21, 28). The activation energy (~8 kcal/mol) for protein antibody complex diffusion is similar to that for the epidermal growth factor-receptor complex on A-431 cells (~6 kcal/mol; [26]).

This discrepancy between lipid and protein diffusion rates most likely means that overall lipid bilayer fluidity is not limiting the rate of diffusion of the antigen-antibody complex in the plasma membrane (see, for example references 1 and 2). This contention is based on the fact that when proteins and peptides are reconstituted into simple artificial bilayers in the "fluid" state, they diffuse at rates approaching lipid probes in similar bilayers, i.e., in the range of 10^{-8} cm^2/s (for reviews, see references 29 and 30). In addition, deliberate alterations of bilayer fluidity, have little or no effect on the lateral diffusion of proteins and lipids (31, 32).

Peripheral constraints to lateral mobility involving the membrane associated cytoskeleton and/or the glycocalyx are almost certainly implicated by these and previous studies (for reviews, see references 2 and 30). Such constraints presumably will be involved in both the retarded diffusion rates as well as the immobile fraction. As noted in the Introduction, the case for cytoskeletal constraints is strong for the lateral diffusion of band 3 proteins in the erythrocyte membrane (3, 4) and is suggestive concerning the mobility of surface proteins in nucleated animal cells (5, 6). The restraints to GP80 lateral mobility are clearly different than those involved in controlling band 3 mobility. First, the mf of GP80, especially at the higher temperatures, is much greater than that for band 3. Second, disruption of the fibroblast spectrin network by microinjection of antispectrin antibodies has no effect on the lateral mobility or mf of GP80 (Mangeat, P., D. O'Dell, K. Burridge, and K. Jacobson, unpublished experiments).

Membrane bound GP80 contains a large, 65,000-dalton extracellular domain (33) that could interact with elements of the extracellular matrix. Little is known of the possible associations of integral membrane glycoproteins with the glycocalyx, but available evidence suggests the interactions may be too localized to play a major role in determining lateral mobility. Immunofluorescence studies on fibroblasts, using antimatrix antibodies (i.e., α-fibronectin, α-collagen, α-proteoglycans) show that the glycocalyx structure is most often fibrillar in nature with coincident staining patterns for the various components often occurring (34, 35). This suggests that relatively large "open" areas with naked plasma membrane exposed could exist unless other proteoglycans and free glycosaminoglycans like hyaluronic acid fill in these spaces and come close to the bilayer surface. Even so, the labeling of many plasma membrane antigens by antibodies suggests easy access of these macromolecular ligands to the plasma membrane through whatever glycocalyx exists. In fact, even large liposomes (36) and erythrocytes (37) can be brought close enough to the plasma membrane of fibroblasts by lectin cross bridging to be subsequently fused by polyethylene glycol treatment. Earlier work (38) indicated that the presence of fibronectin fibrils did not affect the lateral mobility of unspecified surface antigens on fibroblast cell surfaces.

We can speculate on the nature of the peripheral interactions determining the lateral diffusion rates by employing elementary chemical considerations and several assumptions. General treatments (39–41) and a specific, but different, model (42) pertinent to the interpretation of lateral diffusion data have been given previously. We propose that the lateral diffusion behavior of this and other membrane proteins can be described by two populations of diffusing species: one in

rapid exchange with a large set of peripheral binding elements via relatively nonspecific mechanisms and the other in slow exchange with another set of binding elements as shown schematically in Fig. 8. The latter binding would be highly specific; a prototype for these interactions would be the spectrin-ankryin-band 3 complex in erythrocyte membranes (43). The interactions can be described by the following chemical equilibria:

$$A + B \underset{k_r}{\overset{k_f}{\rightleftharpoons}} C \qquad (1a)$$

$$K = [C]/[A][B] \qquad (1b)$$

and,

$$A + B' \underset{k_r'}{\overset{k_f'}{\rightleftharpoons}} C' \qquad (2a)$$

$$K' = [C']/[A][B'], \qquad (2b)$$

where A represents the "free" glycoprotein diffusing in the bilayer, B and B' represent the peripheral binding elements involved in the rapid and slow exchange cases, respectively, and C and C′ represent the glycoprotein-binding element complex in the rapid and slow exchange cases, respectively. The brackets symbolize concentrations and K and K' represent equilibrium constants for the two reactions. The fast exchange reaction described in Eq. 1 is postulated to give rise to the observed diffusive component while the slow exchange reaction (Eq. 2) accounts for the immobile fraction. We first discuss slow diffusion and then turn our attention to an analysis of the immobile fraction.

The case of the retarded protein diffusion rates so often observed in photobleaching studies can be treated in two complementary ways, to a first approximation. Lateral diffusion of the integral glycoproteins is assumed to be limited by transient binding to peripheral structures (i.e., fast exchange) between which the protein takes fast diffusive steps through the bilayer which are governed by membrane fluidity. In the rapid exchange limit,

$$\bar{D} = f_f D_f + f_s D_s, \qquad (3)$$

where $\bar{D}$ is the effective diffusion coefficient and D_f and D_s and f_f and f_s represent the D's and the fractions of the fast and slow diffusing populations, respectively (39). If the unrestricted diffusion coefficient of GP80 in the plasma membrane bilayer is estimated to be 5×10^{-9} cm^2/s (30) and $D_s = 0$, assuming no mobility when the glycoprotein is transiently bound to peripheral elements, then at 25°C only 2.5% of the antigen population exists at a given time as glycoproteins freely diffusing in the bilayer. This is an important implication of the model which is, perhaps, not appreciated at first glance.

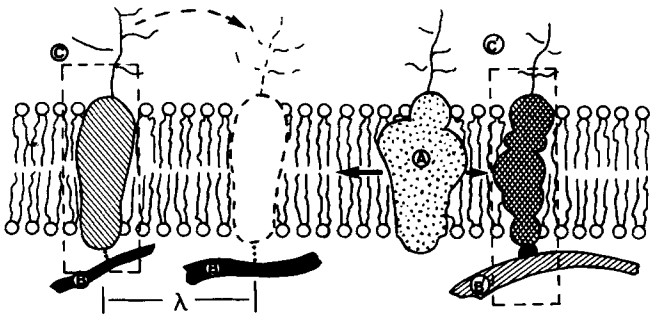

FIGURE 8 Schematic of mobility restraint model. Glycoprotein A corresponds to freely diffusing species A in Eqs. 1 and 2 in text. Complex C is formed when A binds relatively weakly to peripheral structures B; the dotted arrow symbolizes the rapid diffusion step through the bilayer of protein A from one site B to an adjacent one separated by a mean distance, λ. Complex C' is formed when A binds to peripheral element B. These binding elements are depicted on the cytoplasmic side of the plasma membrane but they could also be located on the extracellular surface of the membrane.

Next, to obtain an upper limit on the distance, λ, separating adjacent binding sites (Fig. 8), we can focus on a single diffusing molecule, treating the situation as two dimensional lattice diffusion with

$$\bar{D} = 0.25\nu\lambda^2, \qquad (4)$$

where ν is the jump frequency. In this approximation, ν represents the frequency that complex C dissociates allowing the protein to take a diffusive jump through the bilayer and is equal to τ_{on}^{-1} where τ_{on} represents the lifetime of the complex. We can set expressions 3 and 4 equal in the rapid exchange limit (i.e., $\tau_{on} \ll \tau_{1/2}$, the experimental half-time for FRAP) so that, assuming $D_s = 0$

$$\lambda^2/4\tau_{on} = f_f D_f. \qquad (5)$$

We estimate τ_{off}, the time spent "free" in the bilayer, to be given by the time to diffuse a distance λ to the next peripheral binding element:

$$\tau_{off} = \lambda^2/4D_f, \qquad (6)$$

Substituting Eq. 6 into Eq. 5 for λ yields,

$$f_f = \tau_{off}/\tau_{on}. \qquad (7)$$

That is, the fraction of the entire population that is free at any one instant is equal to the ratio of time a given protein spends freely diffusing in the bilayer versus bound to a peripheral element.[2] Eq. 6 allows calculation of the characteristic distances, λ, as a function of τ_{off}. These distances are subject to the constraints of both the rapid exchange model, namely, that $\tau_{on} \ll \tau_{1/2}$ and that a minimum of $\approx 10^6$ fast exchange binding sites per cell exist. The latter restriction comes from the consideration given above that at any one instant 97.5% of the glycoprotein is bound and that there are $\sim 10^6$ GP80 molecules per cell (8). These conditions set a maximum value for τ_{off} of ~1 ms since this time gives λ of 450 Å (i.e., $\sim 10^6$ sites per 45 × 45 μm cell). (For reference, since a spectrin heterodimer has a length of ~1,000 Å (43), this implies between two and twenty fast exchange binding sites per typical membrane associated cytoskeletal element.) The on time, calculated from Eq. 7, is 40 ms and therefore satisfies the rapid exchange criterion.

One would envision these rapid exchange interactions to be relatively nonspecific and weak. As a possibility, frequent interactions of electronegative actin filaments with positively charged regions of the cytoplasmic domains of transmembrane proteins could provide the general retardation of mobility observed in many photobleaching studies. It should be

[2] A referee has pointed out that this relation also follows from the equilibrium described in Eq. 1 and the rapid exchange condition:

$$f_f = [C]/[A] + [C] = (1 + K[B])^{-1} = k_r/(k_r + k_f[B]);$$

but $k_r = \tau_{on}^{-1}$ and $k_f[B] = \tau_{off}^{-1}$, $f_f = \tau_{on}^{-1}/(\tau_{on}^{-1} + \tau_{off}^{-1}) = [1 + (\tau_{on}/\tau_{off})]^{-1}$. For the case $\tau_{off} \ll \tau_{on}$, $f_f \cong \tau_{off}/\tau_{on}$.

pointed out that the model would equally apply to the case where the interactions that retard diffusion occurred with other membrane proteins that are themselves anchored in the bilayer.

Membrane proteins are postulated to be immobilized by strong interactions with structural elements peripheral to the plasma membranes; in this model, the mobile fraction can be related, with several assumptions, to the equilibrium constant, K', in Eq. $2b$ describing the reaction of membrane proteins, A, with peripheral elements, B', to give tight complexes, C', which are immobile (see Fig. 8). The temperature dependence of this equilibrium will yield a standard enthalpy of reaction, $\Delta H°$, for formation of complex C'. Estimates of the various concentrations in Eq. $2b$ are required to evaluate K'. Since the concentrations of B' and A are not known we take two limiting cases: (a) the total concentration of GP80 molecules, A_0, equals the total concentration of tight binding sites, B_0, and (b) $B_0 \gg A_0$. Furthermore, we assume that in spite of the interactions described in Eq. $1a$ the effective concentration of A is simply A_0 times the mobile fraction since the proteins are hypothesized to be in rapid exchange with peripheral binding sites, B. When $B_0 = A_0$, a quantity proportional to the equilibrium constant, K', may be calculated as $(1 - \text{mf})/(\text{mf})^2$, where mf is the mobile fraction. The linearized data of Fig. 5 allows an approximate standard enthalpy of reaction, Δ H°, to be calculated using the Van't Hoff Isochore. The enthalpy of reaction so calculated is about −18 kcal/mol. If, on the other hand, a large excess of strong binding sites exists ($B_0 \gg A_0$), $K' \propto (1 - \text{mf})/\text{mf}$ and the Δ H° drops to about −12 kcal/mol. Thus, in our model, this range of enthalpies characterizes the relatively strong interaction required to immobilize the antigen-antibody complex for times in excess of the $\tau_{1/2}$ for the FRAP measurement.

Lateral Diffusion Measured in Arbitrary Regions of the Cell Surface

The broad distribution of diffusion coefficients and mobile fractions obtained from synchronous populations of cells is, in itself, striking. One might suppose this to be the result of the spatial resolution (≤ 2 μm) of the spot photobleaching technique allowing investigation of different regions of the cell surface. Several facts contradict this supposition. Following Schlessinger et al. (21) and Edidin and Wei (18), we have compared FRAP determinations at two randomly selected spots on the cell surface. In agreement with the earlier studies we found such comparisons to yield similar data within a factor of about two (Fig. 3); this variation is far less than the range of data seen in Figs. 1 and 2. Furthermore, Petty et al. (16) found a large variation in HLA antigen-antibody mobility data studied by pattern photobleaching, in which the mean diffusion coefficient for the entire cell surface was determined. Similar large variations were found in the mobility of lectin-receptor complexes on neuroblastoma cells (44). These results suggest that cell to cell variation is surprisingly large and that these variations may be global in nature, affecting the entire cell surface, as suggested earlier (45). The structural origin of this heterogenity is unclear at this point.

Lateral Diffusion as a Function of Phase in the Cell Cycle

The broad distribution of D and mf values for synchronous cell populations makes interpretation of possible cell cycle differences difficult. The most striking difference is the depressed mf in G_o cells. Since scanning electron microscope studies show that interphase and G_o cells are relatively flat (46; our data not shown), a villous surface morphology will be a factor only in the interpretation of FRAP data from mitotic cells. Effects on D are likely to be minor based on theoretical arguments (47) and previous experiments (24, 48). Diffusion onto or off of lengthy microvilli could lead to an apparent immobile fraction (48) and possibly explain the generally reduced mf of mitotic cells relative to interphase cells. It should be noted that de Laat et al. (49) did find differences in antigen and lipid probe lateral diffusion as a function of phase in the cell cycle of neuroblastoma cells.

Lateral Diffusion Measured in Specific Regions of the Cell Surface

The spot photobleaching technique offers the capability of studying lateral mobility in selected regions of the cell surface. The antigen was present (see preceding paper) and was partially mobile on the ventral surface, in agreement with earlier studies on generalized cell surface protein labels (50). Thus, proteins, antibody-antigen complexes, and lipids (10) are not inhibited from lateral motion by presence of the substrate, except in specialized regions such as the focal contacts (50). Cell-cell contact in the region where one cell had underlapped another did not affect the mobility of GP80, indicating that there is generally enough clearance between cell and substrate or between two contacting cells to allow the glycoprotein-antibody complex to diffuse in a manner no more restricted than observed on a free cell surface. Possibly, molecules specific for contact zones will be "trapped" (51) in these regions and therefore display a large immobile fraction.

One reproducible difference in lateral diffusion of GP80 on individual cells is that which occurs between the leading and trailing edge (Fig. 7) of motile fibroblasts. According to the scheme given above (see Fig. 8), a reduced affinity for and/or a decreased density of the weak peripheral binding sites, B, which serve to retard lateral diffusion (see Fig. 8), could account for the increased diffusion rate in the leading edge region.

Antibodies directed toward murine cell surface antigens will provide a basis to compare the lateral mobility of various defined components localized to different regions of the plasma membrane (52). Furthermore, it is hoped that determination of changes in lateral diffusion of surface antigens caused by deliberate and characterized biochemical and biological manipulation of cells and their fragments will elucidate in detail those factors governing the lateral mobility and distribution of plasma membrane proteins.

We thank Mr. Bruce Holifield, of the University of North Carolina, for technical assistance. The suggestions of Dr. J. W. Parce, Bowman Grey, School of Medicine, regarding fluorescence fading are gratefully acknowledged. This work was supported by grants NIH GM 29234 (K. Jacobson), American Cancer Society CD-181 (K. Jacobson) and NIH GM 31168 (T. August). K. Jacobson was an Established Investigator of the American Heart Association (77-105) during the conduct of much of this project.

Received for publication 12 December 1983, and in revised form 26 June 1984.

REFERENCES

1. Jacobson, K., E. Elson, D. Koppel, and W. Webb. 1983. International workshop on the application of fluorescence photobleaching techniques to problems in cell biology. *Fed. Proc.* 42:72–79.

2. Jacobson, K., and J. Wojcieszyn. 1981. On the factors determining the lateral mobility of cell surface components. *Comments on Molecular Cellular Biophysics.* 1:189–199.
3. Sheetz, M. P., M. Schindler, and D. E. Koppel. 1980. Lateral mobility of integral membrane proteins is increased in spherocytic erythrocytes. *Nature (Lond.).* 285:510–512.
4. Golan, D. E., and W. Veatch. 1980. Lateral mobility of band 3 in the human erythrocyte membrane studied by fluorescence photobleaching recovery: evidence for control by cytoskeletal interactions. *Proc. Natl. Acad. Sci. USA.* 77:2537–2541.
5. Tank, D. W., Wu, E.-S., and W. W. Webb. 1982. Enhanced molecular diffusibility in muscle membrane blebs: release of lateral constraints. *J. Cell Biol.* 92:207–212.
6. Wu, E.-S., D. W. Tank, and W. W. Webb. 1982. Unconstrained lateral diffusion of concanavalin A receptors on bulbous lymphocytes. *Proc. Natl. Acad. Sci. USA.* 79:4962–4966.
7. Hughes, E. N., and J. T. August. 1981. Characterization of plasma membrane proteins identified by monoclonal antibodies. *J. Biol. Chem.* 256:664–671.
8. Hughes, E. N., G. Mengod, and J. T. August. 1981. Murine cell surface glycoproteins. Characterization of a major component of 80,000 daltons as a polymorphic differentiation antigen of mesenchymal cells. *J. Biol. Chem.* 256:7023–7027.
9. Jacobson, K., Z. Derzko, E.-S. Wu, Y. Hou, and G. Poste. 1977. Measurement of the lateral mobility of cell surface components in single, living cells by fluorescence recovery after photobleaching. *J. Supramol. Struct.* 5:565–576.
10. Jacobson, K., Y. Hou, Z. Derzko, J. Wojcieszyn, and D. Organisciak. 1981. Lipid lateral diffusion in the surface membrane of cells and in multibilayers formed from plasma membrane lipids. *Biochemistry.* 20:5268–5275.
11. Derzko, Z., and K. Jacobson. 1980. Comparative lateral diffusion of fluorescent lipid analogues in phospholipid multilayers. *Biochemistry.* 19:6050–6057.
12. Axelrod, D., D. E. Koppel, J. Schlessinger, E. Elson, and W. W. Webb. 1976. Mobility measurement of analysis of fluorescence photobleaching recovery kinetics. *Biophys. J.* 16:1055–1069.
13. Jacobson, K., Y. Hou, and J. Wojcieszyn. 1978. Evidence for lack of damage during photobleaching measurements of the lateral mobility of cell surface components. *Exp. Cell Res.* 116:179–189.
14. Wolf, D. E., M. Edidin, and P. R. Dragsten. 1980. Effect of bleaching light on measurements of lateral diffusion in cell membranes by the fluorescence photobleaching recovery method. *Proc. Natl. Acad. Sci. USA.* 77:2043–2045.
15. Koppel, D., and M. P. Sheetz. 1981. Fluorescence photobleaching does not alter the lateral mobility of erythrocyte membrane glycoproteins. *Nature (Lond.).* 293:159–161.
15a. Middleton, C. A. 1979. Cell-surface labeling reveals no evidence for membrane assembly and disassembly during fibroblast locomotion. *Nature (Lond.).* 282:203–205.
16. Petty, H. R., L. M. Smith, D. T. Fearon, and H. M. McConnell. 1980. Lateral distribution and diffusion of the C3b receptor of complement, HLA antigens, and lipid probes in peripheral blood leukocytes. *Proc. Natl. Acad. Sci. USA.* 77:6587–6591.
17. Mason, D. W., and A. F. Williams. 1980. The kinetics of antibody binding to membrane antigens in solution and at the cell surface. *Biochem. J.* 187:1–20.
18. Edidin, M., and T. Wei. 1982. Lateral diffusion of H-2 antigens on mouse fibroblasts. *J. Cell Biol.* 95:458–462.
19. Poo, M. 1982. Rapid lateral diffusion of functional Ach receptors in embryonic muscle cell membrane. *Nature (Lond.).* 295:332–334.
20. Axelrod, D., P. Ravdin, D. E. Koppel, J. Schlessinger, W. W. Webb, E. L. Elson, and T. R. Podleski. 1976. Lateral motion of fluorescently labeled acetycholine receptors in membranes of developing muscle fibers. *Proc. Natl. Acad. Sci. USA.* 73:4594–4598.
21. Schlessinger, J. D., D. Axelrod, D. E. Koppel, W. W. Webb, and E. L. Elson. 1977. Lateral transport of a lipid probe and labeled proteins on a cell membrane. *Science (Wash. DC).* 195:307–309.
22. Edidin, M., Y. Zagyansky, and T. J. Lardner. 1976. Measurement of membrane protein lateral diffusion in single cells. *Science (Wash. DC).* 191:466–468.
23. Schlessinger, J., W. W. Webb, E. L. Elson, and H. Metzger. 1976. Lateral motion and valence of F_c receptors on rat peritoneal mast cells. *Nature (Lond.).* 264:550–552.
24. Dragsten, P., P. Henkart, R. Blumenthal, J. Weinstein, and J. Schlessinger. 1979. Lateral diffusion of surface immunoglobulin, Thy-1 antigen and a lipid probe in lymphocyte plasma membranes. *Proc. Natl. Acad. Sci. USA.* 76:5163–5167.
25. Woda, B. A., J. Yguerabide, and J. D. Feldman. 1980. The effect of local anesthetics on the lateral mobility of lymphocyte membrane proteins. *Exp. Cell Res.* 126:327–331.
26. Hillman, G. M., and J. Schlessinger. 1982. Lateral diffusion of epidermal growth factor complexed to its surface receptors does not account for the thermal sensitivity of patch formation and endocytosis. *Biochemistry.* 21:1667–1672.
27. Gall, W. E., and G. M. Edelman. 1981. Lateral diffusion of cell surface molecules in animal cells and tissues. *Science (Wash. DC).* 213:903–905.
28. Eldridge, C. A., E. L. Elson, and W. W. Webb. 1980. Fluorescence photobleaching recovery measurements of surface lateral mobilities on normal and SV40-transformed mouse fibroblasts. *Biochemistry.* 19:2075–2079.
29. Vaz. W. L. C., Z. I. Derzko, and K. A. Jacobson. 1982. Photobleaching measurements of the lateral diffusion of lipids and proteins in artificial phospholipid bilayer membranes. *In* Membrane Reconstitution. G. Poste and G. Nicolson, editors. Elsevier Biomedical Press. 83–136.
30. Jacobson, K. 1983. Lateral diffusion in membranes. *Cell Motility.* 3:367–373.
31. Kleinfeld, A. M., P. Dragsten, R. D. Klausner, W. J. Pjura, and B. D. Matayoshi. 1981. The lack of relationship between fluorescence polarization and lateral diffusion in biological membranes. *Biochem. Biophys. Acta* 649:471–480.
32. Axelrod, D., A. Wight, W. Webb, and A. Horwitz. 1978. Influence of membrane lipids on acetylcholine receptor and lipid probe diffusion in cultured myotube membranes. *Biochemistry.* 17:3604–3609.
33. Hughes, E. N., A. Colombatti, and J. T. August. 1983. Murine cell surface glycoproteins. Purification of the polymorphic Pgp-1 antigen and analysis of its expression on macrophages and other myeloid cells. *J. Biol. Chem.* 258:1014–1021.
34. Hedman, K., S. Johansson, T. Vartio, L. Kjellan, A. Vaheri, and M. Höök. 1982. Structure of the pericellular matrix: association of heparan and chordroitin sulfates with fibronectin procollagen fibers. *Cell.* 28:663–671.
35. Bornstein, P., and J. F. Ash. 1977. Cell surface-associated proteins in connective tissue cells. *Proc. Natl. Acad. Sci. USA.* 74:2480–2484.
36. Szoka, F., K. E. Magnusson, J. Wojcieszyn, Y. Hou, Z. Derzko, and K. Jacobson. 1981. Use of lectins and polyethylene glycol for fusion of glycolipid-containing liposomes with eukaryotic cells. *Proc. Natl. Acad. Sci. USA.* 78:1685–1689.
37. Wojcieszyn, J., R. Schlegel, K. Lumley-Sapanski, and K. Jacobson. 1983. Studies on the mechanism of polyethylene glycol-mediated cell fusion using fluorescent membrane and cytoplasmic probes. *J. Cell Biol.* 96:151–159.
38. Schlessinger, J., L. S. Barak, G. G. Hammes, K. M. Yamada, I. Pastan, W. W. Webb, and E. Elson. 1977. Mobility and distribution of a cell surface glycoprotein and its interaction with other membrane components. *Proc. Natl. Acad. Sci. USA.* 74:2909–2913.
39. Elson, E. L., and J. A. Reidler. 1979. Analysis of cell surface interactions by measurements of lateral mobility. *J. Supramol. Struct.* 12:481–489.
40. Koppel, D. E. 1981. Association dynamics and lateral transport in biological membranes. *J. Supramol. Struct. and Cell Biochem.* 17:61–67.
41. Icenogle, R. D., and E. L. Elson. 1983. Fluorescence correlation spectroscopy and photobleaching recovery of multiple binding reactions. I. Theory and FCS measurements. *Biopolymers.* 22:1919–1948.
42. Koppel, D. E., M. P. Sheetz, and M. Schindler. 1981. Matrix control of protein diffusion in biological membranes. *Proc. Natl. Acad. Sci. USA.* 78:3576–3580.
43. Branton, D., C. M. Cohen, and J. Tyler. 1981. Interaction of cytoskeletal proteins on the human erythrocyte membrane. *Cell.* 24:24–32.
44. Deugnier, M. A., X. Albe, M. Caron, and J. C. Bisconte. 1981. Lateral diffusion of membrane D-galactosyl glycoconjugates of differentiating neuroblastoma cells. *Biochem. Biophys. Res. Commun.* 103:490–497.
45. Edelman, G. M. 1976. Surface modulation in cell recognition and cell growth. *Science (Wash. DC).* 192:218–226.
46. Saxholm, H., and A. Reith. 1979. The surface structure of 7,12-Dimethyl-benz(a) anthracene transformed C3H-10T½ cells. A quantitative scanning electron microscopical study. *Eur. J. Cancer.* 15:843–855.
47. Aizenbud, B. M., and N. D. Gershon. 1982. Diffusion of molecules on biological membranes of nonplanar form. *Biophys. J.* 38:287–293.
48. Wolfe, D. W., A. H. Handyside, and M. Edidin. 1982. Effect of microvilli on lateral diffusion measurements made by the fluorescence photobleaching recovery technique. *Biophys. J.* 38:295–297.
49. de Laat, S. W., P. T. van der Saag, E. L. Elson, and J. Schlessinger. 1980. Lateral diffusion of membrane lipids and proteins during the cell cycle of neuroblastoma cells. *Proc. Natl. Acad. Sci. USA.* 77:1526–1528.
50. Geiger, B., Z. Avnur, and J. Schlessinger. 1982. Restricted mobility of membrane constituents in cell-substrate focal contacts of chicken fibroblasts. *J. Cell Biol.* 93:495–500.
51. Chow, I., and M. M. Poo. 1982. Redistribution of cell surface receptors induced by cell-cell contact. *J. Cell Biol.* 95:510–518.
52. Murphy, T. M., G. Decker, and J. T. August. 1983. Glycoproteins of coated pits, cell junctions, and the entire cell surface revealed by monoclonal antibodies and immunoelectron microscopy. *J. Cell Biol.* 97:533–541.